Phase locking of Josephson-junction series arrays

P. Hadley and M. R. Beasley
Department of Applied Physics, Stanford University, Stanford, California 94305-9040

K. Wiesenfeld
School of Physics, Georgia Institute of Technology, Atlanta, Georgia 30332
(Received 23 March 1988)

We report the results of a stability analysis of coherent oscillations in series arrays of Josephson junctions shunted by a common load. The analysis has found the parameter values for which the coherent, in-phase solution is stable and gives a quantitative measure of the stability. We find that arbitrarily large, dc-biased, arrays of Josephson junctions will phase lock most strongly when the capacitance parameter $\beta_c \approx 1$ and the bias current is about the same as the critical current of the individual junctions. We use bifurcation theory to discuss the role that symmetry plays in determining the form and the stability of these oscillations. Simulations with up to 100 junctions confirm the results of the stability analysis. Arrays of nearly identical junctions are also discussed.

INTRODUCTION

Josephson junctions have the remarkable property that they oscillate at a frequency that is proportional to the voltage across the junction.[1] Connecting multiple Josephson junctions together in a series array introduces the possibility that the junctions will phase lock and oscillate coherently.[2] Understanding the mechanisms that are responsible for such phase locking is an interesting problem of nonlinear dynamics as well as being useful for practical applications. We present here analysis and numerical simulations that detail these phase-locked solutions and their stability.

From the point of view of applications, Josephson junction arrays are of considerable interest as local oscillators, mixers, and parametric amplifiers in microwave and millimeter-wave circuits.[3] Arrays have the advantage over single junctions that their power and source impedance can be increased to practically useful levels.[4] Typically for these applications, the junctions are arranged in a one-dimensional array shunted by a load. This is the configuration that we consider here.

The conditions under which arrays of Josephson junctions phase lock has been analyzed using perturbative techniques by Jain, Likharev, Lukens, and Sauvageau.[3] While extremely useful, their analysis is restricted to a limited range of parameters. Here we employ an exact, albeit numerical approach based on Floquet theory to examine the stability of the in-phase coherent oscillations under general conditions. This technique is similar to one that was used to study the stability of single Josephson junction circuits.[5] By in-phase we mean that all of the junctions oscillate identically. We plot the numerical results for a variety of cases of practical interest. Throughout this paper we employ a lumped parameter model for the circuit which is valid for arrays small compared to a wavelength of the radiation and for distributed arrays. Within this model we show that arbitrarily large arrays of junctions will phase lock and oscillate in phase and we quantify how stable the in-phase oscillations are. Using symmetry arguments we show that when the in-phase oscillations lose stability as many as $(N-1)!$ new, symmetry-related solutions can appear. The solutions that appear after the in-phase solution has lost stability also show some degree of coherence although the junctions no longer all oscillate identically. Numerical simulations of these other solutions are presented.

BASIC CIRCUIT AND MODEL

The general circuit diagram of the array we are considering is shown in Fig. 1. It is a series array of current biased Josephson junctions shunted by a load impedance. In this circuit the oscillating voltage across the junctions generates a high-frequency load current. This current flows through all of the junctions and serves to couple them. Under certain conditions the interaction between the oscillating load current and the oscillating supercurrent flowing through the junctions leads to phase locking and coherent oscillation of each junction in the array.

The behavior of Josephson junctions is commonly modeled using the shunted-junction model.[6,7] Within this model the equations that describe the behavior of the circuit in Fig. 1 are

$$\beta_c \ddot{\phi}_k(t)+\dot{\phi}_k(t)+\sin[\phi_k(t)]+I_L(t)=I_B \qquad k=1,2,\ldots,N \quad (1a)$$

$$V(t)=\sum_{k=1}^{N}\dot{\phi}_k(t)=F(I_L(t)) \; . \quad (1b)$$

The first equation is a statement of the conservation of current and the second that the voltage across the array of junctions equals the voltage across the load. We have used the usual reduced units, measuring current in units of the critical current I_c voltage in units of I_cR_N, resistance in units of R_N, capacitance in units of $\hbar/(2eI_cR_N^2)$, inductance in units of $\hbar/(2eI_c)$, and time in units of

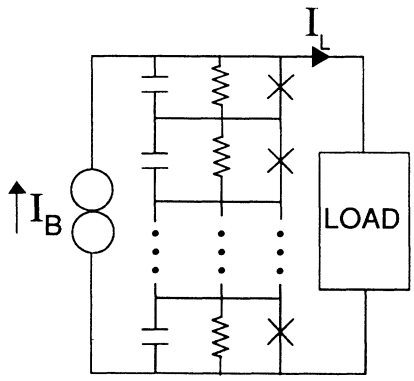

FIG. 1. Circuit diagram of a series Josephson junction array shunted by a load impedance.

$\hbar/2eI_cR_N$. Here N is the number of junctions, R_N is the appropriate shunt resistance of the junctions, $\beta_c = (2eI_cR_N^2C_j)/\hbar$ is a dimensionless measure of the capacitance C_j of the junctions, I_L is the load current, I_B is the applied bias current, and $F(I_L)$ is the functional that relates the load current I_L to the total voltage V across the array. (For instance when the load in Fig. 1 is a capacitor $F(I_L)=(1/C)\int I_L\,dt$.) The ϕ_k's are the differences in the phases of the quasiclassical, superconducting wave functions on the two sides of the junctions. This model is a good approximation over a wide range of β_c, including weak-link superconductor–normal-metal– superconductor (S-N-S–type) junctions where $\beta_c \ll 1$, shunted tunnel junctions ($\beta_c \approx 1$), and unshunted tunnel junctions at voltages below the energy gap ($\beta_c \gg 1$).

For the in-phase solution all of the junctions oscillate together, $\phi_k = \phi_0$. In this case the $N+1$ equations for the array reduce to just two equations,

$$\beta_c\ddot{\phi}_0(t)+\dot{\phi}_0(t)+\sin[\phi_0(t)]+I_L(t)=I_B \tag{2a}$$

$$V(t)=N\dot{\phi}_0(t)=f(I_L(t))\ . \tag{2b}$$

This is equivalent to the equations for a single junction shunted by a load with a scaled load functional $f(I)=F(I)/N$. Thus the calculation of the in-phase solution for an arbitrarily large array reduces to the equivalent calculation for a single junction.

STABILITY ANALYSIS OF THE IN-PHASE STATE

To determine the stability we consider small perturbations to the in-phase solution, $(\phi_k=\phi_0+\eta_k, I=I_L+i)$. Linearizing around the in-phase solution results in a set of linear differential equations with periodic coefficients,

$$\beta_c\ddot{\eta}_k(t)+\dot{\eta}_k(t)+\cos[\phi_0(t)]\eta_k(t)+i(t)=0 \qquad k=1,2,\ldots,N \tag{3a}$$

$$\sum_{k=1}^{N}\dot{\eta}_k(t)=F'(I_L(t))i(t) \tag{3b}$$

where $\phi_0(t)$ and $I_L(t)$ are functions of period T that solve Eq. (2). $F'(I_L(t))i(t)$ is shorthand for the first-order term in the expansion of the load functional $F(I_L+i)$ linearized about the in phase load current I_L.

We can greatly simplify the linearized equations by taking advantage of the permutation symmetry of the system. (Any permutation, $\eta_j \leftrightarrow \eta_k$, leaves Eq. (3) unchanged.) We transform to the natural coordinates of this system, which are the mean coordinate $\varphi=(1/N)\sum_{k=1}^{N}\eta_k$, and the $N-1$ relative coordinates, $\zeta_k=\eta_k-\eta_{k+1}$. The Eqs. (3) then become,

$$\beta_c\ddot{\zeta}_k(t)+\dot{\zeta}_k(t)+\cos[\phi_0(t)]\zeta_k(t)=0, \quad k=1,2,\ldots,N-1 \tag{4a}$$

$$\beta_c\ddot{\varphi}(t)+\dot{\varphi}(t)+\cos[\phi_0(t)]\varphi(t)+i(t)=0\ , \tag{4b}$$

$$N\dot{\varphi}(t)=F'(I_0(t))i(t)\ . \tag{4c}$$

This transformation decouples all N coordinates in the problem. Further simplification results because all of the relative coordinates obey the same equation. Thus, because of symmetry, the stability analysis of the original $N+1$ equations reduces to solving the above set of three equations. The in-phase solution ϕ_0 will remain stable as long as the relative coordinates do not grow. We therefore focus our attention on Eq. (4a).

Equation (4a) arises in many physical problems and can be analyzed using Floquet theory.[8] The analysis shows that any solution to this equation can be expressed as a linear combination of two fundamental solutions, $\zeta_a(t)$ and $\zeta_b(t)$, which are specified by the initial conditions: $\zeta_a(0)=1$, $\dot{\zeta}_a(0)=0$, $\zeta_b(0)=0$, $\dot{\zeta}_b(0)=1$. Since $\cos(\phi_0)$ is a periodic function, $\zeta_a(t+T)$ and $\zeta_b(t+T)$ must also be solutions to Eq. (4a), which can be expressed in terms of $\zeta_a(t)$ and $\zeta_b(t)$. This leads to the vector equation,

$$\begin{bmatrix}\zeta_a(t+T)\\ \zeta_b(t+T)\end{bmatrix}=\begin{bmatrix}\zeta_a(T) & \dot{\zeta}_a(T)\\ \zeta_b(t) & \dot{\zeta}_b(T)\end{bmatrix}\begin{bmatrix}\zeta_a(t)\\ \zeta_b(t)\end{bmatrix}\ . \tag{5}$$

The eigensolutions of Eq. (5) are called the Floquet solutions and can be put in the form $\zeta_1=e^{\rho_1 t}\chi_1(t)$, $\zeta_2=e^{\rho_2 t}\chi_2(t)$, where $\chi_1(t)$ and $\chi_2(t)$ are periodic functions of period T and $\rho_1+\rho_2=-1/\beta_c$. The ρ's are called the Floquet exponents and their real parts determine the stability of the perturbations. They are related to the eigenvalues λ_j of the matrix in Eq. (5) by $\rho_j=\ln(\lambda_j)/T$. If both $\mathrm{Re}(\rho_1)$ and $\mathrm{Re}(\rho_2)$ are negative, then any initial perturbation decays and the in-phase solution is linearly stable. If either exponent has a positive real part, the perturbations grow and the in-phase solution is linearly unstable. Finally if either $\mathrm{Re}(\rho_1)=0$ or $\mathrm{Re}(\rho_2)=0$, then the perturbations to Eq. (4) neither grow nor decay: We then say that the in-phase state is (linearly) neutrally stable, and nonlinear terms omitted in writing Eq. (3) determine the ultimate stability of $\phi_0(t)$. Note that the imaginary part of the Floquet exponents are determined only up to an integer multiple of $2\pi i/T$. To avoid any ambiguity we will pick $-\pi/T < \mathrm{Im}(\rho) \le \pi/T$.

Before discussing the numerical solutions to these equations we consider approximate solutions for the Floquet exponents in various limits. The approximate solu-

tions give physical insight and they also provide a check on our numerical work. When $\cos(\phi_0)$ oscillates with a period much shorter than any other time in the problem we can employ the averaging method[9] to find an approximate solution to Eq. (4a). In this approximation, which is valid for $\beta_c \gg T \approx 2\pi/I_B$, we replace $\cos(\phi_0)$ with its average value, $\langle \cos(\phi_0) \rangle$. The solutions to the averaged equation are

$$e^{\rho_+ t} \text{ and } e^{\rho_- t}$$

where

$$\rho_\pm = \frac{-1 \pm [1 - 4\beta_c \langle \cos(\phi_0) \rangle]^{1/2}}{2\beta_c} . \tag{6}$$

For $I_B \gg 1$, $\cos(\phi_0)$ is nearly sinusoidal and $\rho_+ \approx -\langle \cos(\phi_0) \rangle \to 0$. Hence, the in-phase solution is stable for $\langle \cos(\phi_0) \rangle > 0$ and approaches neutral stability as the bias current increases. For $\beta_c \gg 1$, the in-phase solution again approaches neutral stability as the largest real part of the Floquet exponents is bounded by $1/\sqrt{\beta_c} > \rho_+ > -1/(2\beta_c)$. Therefore we conclude that arrays of junctions with $\beta_c \gg 1$, or $I_B \gg 1$ will not phase-lock strongly.

In the highly damped limit one can take $\beta_c = 0$ and the equation for the relative coordinate can be solved exactly. Direct integration of Eq. (4a) in this case yields,

$$\zeta(t) = \exp\left[-\int_0^t \cos[\phi_0(t')] dt' \right] . \tag{7}$$

From this solution we see that such an array will once again phase lock when $\langle \cos(\phi_0) \rangle > 0$. By differentiating Eq. (2a) in this case one finds

$$\cos(\phi_0) = \frac{-1}{T} \int_0^T \frac{\dot{I}_L(t)}{\dot{\phi}_0(t)} dt . \tag{8}$$

Except for bias currents close to the critical current both $I_L(t)$ and $\dot{\phi}_0(t)$ are nearly sinusoidal, periodic functions. Here $\dot{\phi}_0(t)$ is the voltage across the load and $I_L(t)$ is the current through the load so $I_L(t)$ leads $\dot{\phi}_0(t)$ by $\pi/2$ when the load is capacitive, $I_L(t)$ lags $\dot{\phi}_0(t)$ by $\pi/2$ when the load is inductive, and $I_L(t)$ has the same phase as $\dot{\phi}_0(t)$ when the load is resistive. These phase relationships taken together with Eq. (8) dictate the sign of $\langle \cos(\phi_0) \rangle$ and show that in this limit ($\beta_c = 0, I_B \gg 1$) the junctions will phase lock with an inductive load, will not phase lock with a capacitive load, and will be neutrally stable with a resistive load. This agrees with the earlier perturbation calculation of Jain, Likharev, Lukens, and Sauvageau,[3] and with our numerical results in this limit which we present in the next section.

APPLICATIONS OF THE STABILITY ANALYSIS

As we discussed at the beginning of the paper, it is only by virtue of the existence of a load that the junctions can couple. Therefore it is of interest to examine the nature of the stability of the in-phase state for various typical loads. We have done this for six representative cases which include a resistive load, a capacitive load, two inductive loads, and series and parallel resonant inductance-capacitance (LC) loads. The Floquet exponents were calculated in each case by numerically determining $\zeta_a(t)$, $\zeta_b(t)$, and $\phi_0(t)$ by means of a Runge-Kutta algorithm and then using these results to diagonalize the matrix of Eq. (5). Each time the matrix was diagonalized, a check was performed to insure that $|\lambda_1\lambda_2 - e^{-T/\beta_c}|$ was less than 0.05. The condition, $\lambda_1\lambda_2 - \epsilon^{-T/\beta_c} = 0$, is equivalent to $\rho_1 + \rho_2 = -1/\beta_c$ which is a result of Floquet theory. When the period of the oscillation gets long ($T \gg 1$), as does happen for bias currents near the critical current, longer numerical integrations are required and it becomes more difficult to calculate the Floquet exponents. In fact for low bias currents the condition, $\mathrm{Re}(\rho_+) > -1/(2\beta_c)$, is violated in Figs. 2(a) and 2(b) although the numerical results are within the limits stated above.

In Figs. 2(a)–2(f) we plot contours of the largest real part of the Floquet exponents associated with the relative coordinate as a function of the junction capacitance β_c and the bias current I_B for each of these loads. These stability plots show the range of parameters over which the in-phase solution is stable and they provide a quantitative measure of the stability. The heavy line is the $\mathrm{Re}(\rho) = 0$ contour and separates the stable and unstable regions. The dashed line corresponds to the transition to the zero voltage state. To the left of this line the junctions no longer oscillate and questions concerning coherent oscillations are moot. The in-phase solution is most stable for the regions where the exponents are most negative. For instance an exponent of -0.4 corresponds to the perturbations decreasing by a factor of about 10 for every cycle of the in-phase oscillations. As the figures indicate we have observed stable in-phase oscillations in some region of the β_c-I_B plane for each type of load. Universally the strongest phase locking occurs for β_c in the range 0–1 and I_B in the range 1–2. Lee and Schwarz found similar results for the optimum phase-locking regime based on calculations for two junction arrays.[10] These plots relate the stability of arbitrarily large arrays of junctions with a load that scales with the number of junctions. For instance Fig. 2(a) relates the stability of a series array of N junctions shunted by a resistor whose resistance is $R = N$ in our reduced units. The appropriate scalings for the other circuits are given in the figure caption.

Figures 2(a) and 2(b) show that in-phase oscillations are stable in most of the $\beta_c - I_B$ plane when the load is resistive or capacitive. The stability plots for the inductive loads, Figs. 2(c)–2(d), are nearly the complement of the stability plot for the capacitive load or resistive load. (In the circuit of Fig. 2(d) a large capacitor is included in series with the inductor to block dc currents which would short the junctions, but the load appears inductive at all relevant frequencies.) Roughly speaking, the in-phase oscillations are stable for inductive loads in the regions where they were unstable for capacitive loads. As β_c or I_B (or both) become large the real part of the Floquet exponent approaches zero in all of these plots implying that the in-phase state approaches neutral stability. In this

limit, arrays with a resistive or capacitive loads are stable and approaching neutral stability while arrays with inductive loads are unstable and approaching neutral stability. The numerical results agree with the limiting expressions presented above in all of the limits discussed. We emphasize, however, in the $\beta_c = 0$, $I_B \gg 1$ limit our numerical work shows that the range of β_c for which these limiting results are quantitatively valid is rather narrow.

The behavior of the stability of the in-phase solutions as the load goes through a resonance is shown in Figs. 2(e)–2(f). For low bias currents the circuit in Fig. 2(e) has a capacitive impedance and the stability plot resembles that of the simple capacitive load, Fig. 2(b). For high bias currents the circuit in Fig. 2(e) has an inductive impedance and the stability plot resembles that of the simple inductive load, Fig. 2(c). Analogous statements can be made about the limiting regions in Fig. 2(f). This

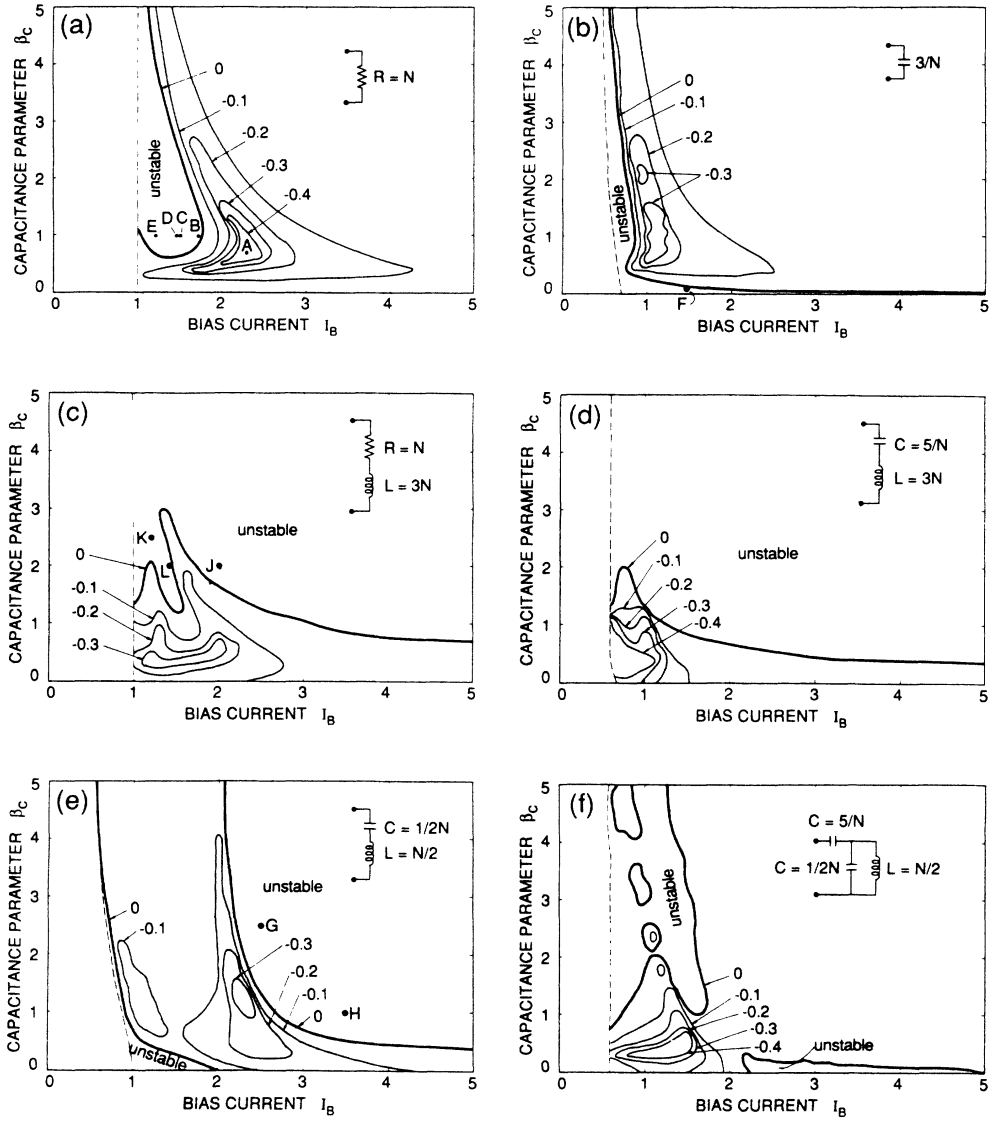

FIG. 2. Contours of the largest real part of the Floquet exponents are plotted as a function of the junction capacitance β_c and the bias current I_B. The in-phase solution is unstable for $\mathrm{Re}(\rho) > 0$ and is most stable for the most negative exponents. These plots relate the stability of arrays with an arbitrarily large number of junctions where the impedance of the load scales with the number of junctions. (a) Resistive load with an impedance matched to the impedance of the array $R = N$. (b) Capacitive load $C = 3/N$. (c) Load is a series resistor inductor, $R = N, L = 3N$. (d) Load is a series inductor capacitor, $L = 3N, C = 5/N$. Here a large capacitor is used to block dc currents which would short the junctions. The load has an inductive impedance at all relevant frequencies. (e) Load is a series inductor capacitor which passes through a resonance at a bias current of about 2, $L = N/2, C = 1/(2N)$. (f) Load is a parallel inductor-capacitor with a large blocking capacitor to prevent the inductor from shorting the junctions, $L = N/2, C = 1/(2N)$, blocking capacitor $= 5/N$. This load also passes through a resonance at a bias current of about 2.

shows how one can piece together the approximate stability plots of more complicated circuits by taking parts of simpler circuits in the appropriate limits.

STABILITY LOSS BY IN-PHASE OSCILLATIONS

The manner in which the in-phase solution loses stability depends to a large extent on the symmetries of the governing circuit equations. The relationship between symmetry and stability can best be described using the language of bifurcation theory.[11] A solution loses stability when at least one Floquet exponent crosses into the right half-plane. Such an event is called a bifurcation, and signals an abrupt change in the dynamics. In the absence of special constraints or any underlying symmetry, there are only three ways in which the solution can lose stability as a single parameter is varied [see Fig. 3(a)]. The three possibilities are a saddle node bifurcation, where a single exponent crosses the imaginary axis at $\mathrm{Im}(\rho)=0$, a period doubling bifurcation, where a single exponent crosses the imaginary axis at $\mathrm{Im}(\rho)=\pi/T$, and a Hopf bifurcation, where a complex-conjugate pair of exponents cross the imaginary axis anywhere else.

When an underlying symmetry is present, however, these are not the only generic bifurcations, since typically one can have several exponents crossing into the right half-plane simultaneously.[12] In the present array problem, there is a permutation symmetry; any transformation of Eq. (1) which exchanges two junctions leaves the circuit equations unchanged. It follows that if $(\phi_1,\phi_2,\ldots,\phi_j,\phi_k,\ldots,\phi_N)$ is a solution then so is $(\phi_1,\phi_2,\ldots,\phi_k,\phi_j,\ldots,\phi_N)$, as are all of the other $N!$ permutation related solutions. Of course, all of these solutions may not be distinct. If all $N!$ permutations give the same solution, then we call this a symmetric solution; this is just what we have been calling the in-phase solution. On the other hand, if a solution is not invariant with respect to all $N!$ permutations of the $\{\phi_k\}$, then we call it a symmetry-broken solution.

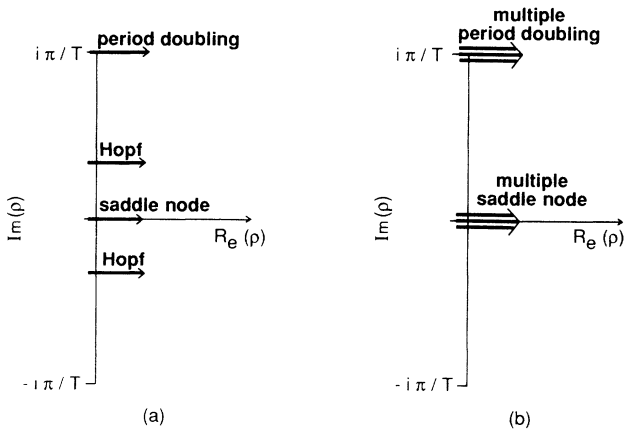

FIG. 3. (a) The three generic, codimension-1 bifurcations (period-doubling, saddle-node, and Hopf) occur as single Floquet exponents cross the imaginary axis at $i\pi/T,0$, and as a complex-conjugate pair respectively. (b) Two multiple bifircations in which many Floquet exponents cross the imaginary axis together were observed at $\mathrm{Im}(\rho)=\pi/T$ and $\mathrm{Im}(\rho)=0$.

We are interested first and foremost in the instabilities suffered by the in-phase (symmetric) solution; there are two distinct possibilities. First, the instability can give rise to a new solution which is also in phase, so that the entire nonlinear problem reduces to Eq. (2), which has no underlying symmetry. Consequently, the symmetry plays no role, and we expect to find only the generic bifurcations listed above. This happens when one of the Floquet exponents associated with Eqs. (4b) and (4c) crosses into the right half-plane while the Floquet exponents associated with Eq. (4a) have negative real parts. The other possibility is that the system undergoes a symmetry-breaking bifurcation, in which case the new solutions no longer represent in-phase oscillations of the array. In this case a Floquet exponent associated with Eq. (4a) crosses into the right half-plane and the underlying symmetry plays an important role in the observed dynamics. The general topic of the effects of symmetry on the bifurcation structure of nonlinear dynamical systems is under intense investigation,[11] but the current understanding is not nearly so complete as the symmetry-free situation. Indeed, very little formal work has been reported on the (permutation) symmetry relevant to the present problem.

We turn first to the simplest case, namely arrays consisting of only two junctions. We have observed two of the generic bifurcations (period doubling and saddle node) as well as symmetry breaking. To help visualize how the in-phase state loses stability in each of these cases we have made phase portraits for the dynamics at various points in the stability plots [Figs. 4(a)–4(f)]. These phase portraits are projections of the circuit's phase space trajectories onto the $\sin(\phi_1)$-$\sin(\phi_2)$ plane. Physically, the phase portraits can be interpreted as plots of the supercurrents of the two junctions but we prefer to

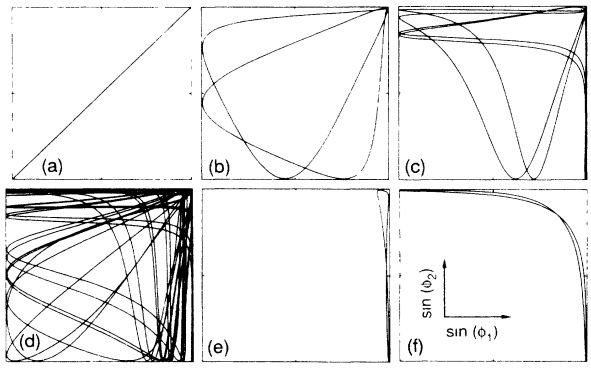

FIG. 4. These phase portraits are projections of the two-junction-array trajectory in phase space onto the $\sin(\phi_1)$-$\sin(\phi_2)$ plane. (a) In-phase solution recorded at the point labeled A in Fig. 2(a), $I_B=2.3$, $\beta_c=0.75$. (b) Solution with twice the period of the in-phase oscillations recorded at the point labeled B in Fig. 2(a), $I_B=1.7$, $\beta_c=1$. (c) Solution with four times the period of the in-phase oscillations recorded at the point labeled C in Fig. 2(a), $I_B=1.5$, $\beta_c=1$. (d) Chaotic solution recorded at the point labeled D in Fig. 2(a), $I_B=1.45$, $\beta_c=1$. (e) Symmetry-broken solution recorded at the point labeled E in Fig. 2(a), $I_B=1.2$, $\beta_c=1$. (f) Antiphase solution recorded at the point labeled F in Fig. 2(b), $I_B=1.2$, $\beta_c=0.1$.

think of them as two-dimensional windows looking into phase space that allow us to infer the symmetry and topology of the solutions. The letters on the stability plots correspond to the parameter values for which the phase portraits were made. For instance, Fig. 4(a) is a phase portrait of the dynamics of a two-junction array which has the parameter values corresponding to the point labeled A in Fig. 2(a). In this case the phase portrait is a diagonal line stretching from $[-1,-1]$ to [1,1], corresponding to an in-phase solution ($\phi_1=\phi_2$). Phase portraits such as this are observed throughout the stable regions of the stability plots, as expected.

Figure 4(b) is a phase portrait of the dynamics at the point labeled *B* at the edge of the unstable region in Fig. 2(a). Here a Floquet exponent has crossed the imaginary axis at $\mathrm{Im}(\rho)=\pi/T$ and the in-phase solution has undergone a period-doubling bifurcation. Notice that the period-doubled solutions makes two loops in phase space before repeating itself and thus has twice the period of the in-phase solution. (The curve can intersect itself since it is only a projection of the true, nonintersecting trajectory onto the plane.) This solution is coherent in the sense that there is a definite (time-dependent) phase relationship between the oscillations of the two junctions but they do not oscillate identically as they do in the in-phase solution. Moving further into the unstable region to point *C*, a second period-doubling occurs and the solution has four times the period of the (unstable) in-phase state [Fig. 4(c)]. Further decreasing of the bias current leads to a cascade of period-doubling bifurcations and to chaos [Fig. 4(d)]. Moving back toward the stability boundary to point *E* we observe a symmetry-broken solution [Fig. 4(e)]. This solution does not share the permutation symmetry of the governing equations; indeed $\phi_1(t)$ and $\phi_2(t)$ have different wave forms altogether, though they do have the same period.

When the in-phase solution of a two-junction array loses stability via a saddle-node bifurcation a different solution appears. A phase portrait of this new solution, for the point labeled *F*, is shown in Fig. 4(f). This is the antiphase solution which was discussed by us previously.[13] In the antiphase state all of the junctions oscillate at the same frequency but they each have a distinct phase. The phases interfere destructively in such a way that the fundamental of the supercurrent oscillations vanishes. In that earlier work we showed that the antiphase state can itself lose stability via further symmetry breaking, leading to period-doubling bifurcations and chaos.

Elsewhere in the stability plots of Fig. 2 we observed the antiphase solution at the points labeled *G*, *H*, and *J*. A symmetry-broken solution was observed at the point labeled *K*, and chaotic solution was observed at *L*.

We now move on to arrays containing more than two identical junctions. In this case, the Floquet exponents are degenerate. More precisely, since the $N-1$ Eqs. (4a) that govern the relative coordinates are identical, the $N-1$ associated exponents are all equal, and these exponents all cross the imaginary axis simultaneously. In our simulations we have observed multiple Floquet exponents cross the imaginary axis at $\mathrm{Im}(\rho)=0$ and at $\mathrm{Im}(\rho)=\pi/T$: We will call such an event a multiple bifurcation. A multiple bifurcation in which identical sets of complex conjugate pairs of eigenvalues cross the imaginary axis simultaneously was never observed.

Our simulations show that when the in-phase state loses stability via a multiple bifurcation at $\mathrm{Im}(\rho)=0$ the array assumes a symmetry broken, antiphase solution (the fundamental of the supercurrent oscillations vanishes). Figure 5(a)–5(f) shows snapshots of the phases ϕ_k of two, three, four, five, six, and ten junction arrays in the antiphase solution at eight points in a cycle. These snapshots were made at point *G* of Fig. 2(e). The phases are measured as angles from vertical as they would be in the pendulum analogy to Josephson junctions.[7] Viewed successively from left to right the snapshots form a movie of the antiphase solution. Note how the phases are spread out, tending to add destructively in this solution. In contrast to the two junction case of Fig. 5(a), the solutions shown in Fig. 5(b)–5(f) are symmetry-broken solutions; they do not have the full symmetry of the equations. Consequently, any transformation that permutes two of the junctions will usually generate new, symmetry-broken solutions. Since each junction has a distinct phase in the antiphase solution, it follows that at least $(N-1)!$ solutions are created when the $N-1$ exponents cross the imaginary axis at $\mathrm{Im}(\rho)=0$ and the system enters the antiphase solution.

A different type of solution appears for a multiple bifurcation at $\mathrm{Im}(\rho)=\pi/T$. In this case we observe both a period doubling and symmetry breaking at the bifurcation point. The observed solution has twice the period of the in-phase solution and the phases of the junctions

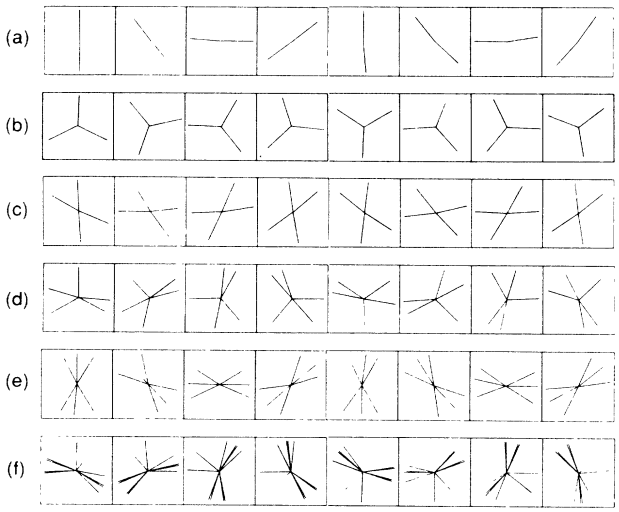

FIG. 5. Six sets of snapshots of the phases ϕ_k of an *N*-junction array in the antiphase solution at eight points in a cycle. The phases are measured as angles from vertical as they would be in the pendulum analogy to Josephson junctions. Viewed successively from left to right the snapshots form a movie of the antiphase solution. Note that the phases tend to add destructively in this solution. The load in each case was a series inductor-capacitor where $L=N/2$, $C=1/(2N)$, $I_B=2.5$, $\beta_c=2.5$, where N is the number of junctions. (a) $N=2$. (b) $N=3$. (c) $N=4$. (d) $N=5$. (e) $N=6$. (f) $N=10$.

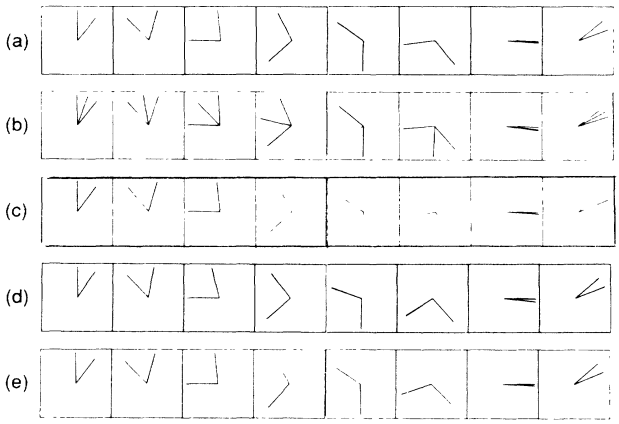

FIG. 6. Illustration of the solution that appears after a multiple bifurcation where many eigenvalues cross the imaginary axis at $\mathrm{Im}(\rho)=\pi/T$. This solution has twice the period of the in-phase solution. For more than three junctions the phases form coherent subgroups and half of the junctions oscillate with one phase while half oscillate with another. The load in this case is a resistor, $R=N$, $I_B=1.7$, $\beta_c=1$. (a) $N=2$. (b) $N=3$. (c) $N=4$. (d) $N=5$. (e) $N=50$. (a) is the same solution as that depicted in Fig. 4(b).

divide into a small number of coherent subgroups. Arrays with even numbers of junctions form two groups where half of the junctions oscillate with one phase and half oscillate with another. Odd-numbered arrays with greater than three junctions also form two groups, dividing themselves as evenly as possible. The case of three junctions seems to be a special case, with all three junctions out of step. Figures 6(a)–6(e) illustrate the behavior for arrays of two, three, four, five, and 50 junctions. Notice that for arrays of four or more junctions the solutions look very much like the two-junction case, even for as many as 50. This solution has somewhat lower symmetry than the full permutation symmetry of the equations. In fact, this multiple bifurcation yields $N!/[\alpha!(N-\alpha)!]$ new, symmetry related solutions, where α is the integer part of $N/2$. In the large-N limit, 2^N new solutions appear.

Thus the consequence of having many Floquet exponents cross the imaginary axis simultaneously seems to be a tremendous increase in the number of new solutions that appear. This phenomena has been termed "attractor proliferation," and seems to be a common occurrence in dynamical systems with many coupled degrees of freedom, including nonlinear oscillator arrays.[14]

NONIDENTICAL JUNCTIONS

Thus far we have dealt with the idealized case of identical junctions in order to make the problem tractable for arrays with arbitrarily large numbers of junctions. The hope is that when there are just small parameter mismatches these results will remain qualitatively valid. To determine the effect that nonidentical junction parameters have on the in-phase oscillations we have performed simulations of 100 junction arrays which would have phase locked strongly if all the junctions were identical. Figures 7(a)–7(e) are movies of nonidentical junction arrays in which we have introduced flat distributions of 0%, 5%, 10%, 15%, and 20% in the critical currents, the shunt resistances and the capacitances of the junctions. The lengths of the lines that show the positions of the phases are proportional to the critical currents of the junctions. Thermal noise was also included in the simulations. When the noise terms are included in Eq. (1) we have,

$$\beta_c\ddot{\phi}_k(t)+\dot{\phi}_k(t)+\sin[\phi_k(t)]+I_L(t)=I_B+\xi_k(t) \qquad k=1,2,\ldots,N \quad (9a)$$

$$V(t)=\sum_{k=1}^{N}\dot{\phi}_k(t)=F(I_L(t))\ , \quad (9b)$$

where $\xi_k(t)$ are the uncorrelated noise currents, $\langle\xi_k(t)\xi_{k'}(t')\rangle=(4/\gamma)\delta_{kk'}\delta(t-t')$, and $\gamma=\hbar I_c/(ek_BT)=1150$. This level of thermal noise corresponds to critical currents of 10^{-4} A and an operating temperature of 4.2 K. Notice that the oscillations remain largely in phase when a 15% spread in the junction parameters is introduced. The main effect of the spread in the phases is to reduce the net amplitude of the in-phase oscillation. These simulations show that the in-phase solution remains stable when modest junction mismatches and thermal noise are included.

As for stability, intuitively we expect that for the nonidentical junction case the Floquet exponents would no longer be identical but rather they would be scattered around the identical junction value. This scattering implies that some of the exponents would have greater real parts than in the identical junction case. Since the in-phase solution loses stability when any one of the exponents crosses the imaginary axis, the scattering of the exponents due to nonidentical junctions would make the

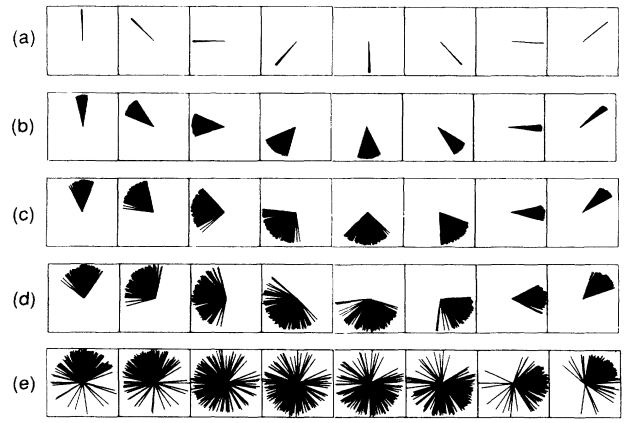

FIG. 7. Illustration of the solution for 100 junction arrays with nonidentical parameters and a matched resistive load $R=N$. Each sequence has a different percentage spread in the junction parameters (critical current, capacitance, and shunt resistance). (a) 0% spread in the junction parameters. (b) 5%. (c) 10%. (d) 15%. (e) 20%. In each case $I_B=2.3$, $\beta_c=0.75$, and $\gamma=1150$.

in-phase solution less stable. The simulations agree with this picture qualitatively but a quantitative numerical study of this effect has not been made. For another discussion of nonuniform arrays see the work of Sauvageau, Jain, and Lukens.[15]

OTHER APPLICATIONS

Although the numerical work was done for circuits which might have applications as local oscillators, the limiting form for the Floquet exponents for other circuits involving series arrays of Josephson junctions can be determined as well. In particular, series arrays of Josephson junctions have been used to build parametric amplifiers[6] and voltage standards[16] in which each of the junctions interacts with an external signal. In terms of the variables used in this paper this is equivalent to making the bias current I_B in Eq. (1) time dependent. In this case the in-phase solution still exists and the solutions to Eq. (3) still determine the stability of the in-phase solution. The only difference is that the in-phase solution ϕ_0 depends on the now time-dependent bias current. The limiting form for the Floquet exponents in a practically important limit $\beta_c \gg 1$ still applies, namely $1/\sqrt{\beta_c} > \rho_+ > -1/(2\beta_c)$. Thus the junctions will not mutually phaselock strongly and the in-phase state will approach neutral stability for large β_c for these circuits as well.

CONCLUSIONS

We have presented a general approach to the stability analysis of series arrays of Josephson junctions. By taking advantage of the symmetry in the problem we were able to determine the stability of the in-phase solution for arrays with an arbitrarily large number of junctions. Applying this analysis to a variety of loads, β_c's and bias currents, we find empirically that in the in-phase solution is most stable when $\beta_c \approx 1$ and the bias current is on the order of the critical current of the junctions. We showed that the in-phase solution can lose stability via a multiple bifurcation and that as many as $(N-1)!$ new solutions can appear. This analysis should prove useful both in the design of practical array circuits and as an example of the types of dynamics that can occur in high-dimensional nonlinear systems.

ACKNOWLEDGMENTS

We would like to thank Anlage for a very helpful reading of the manuscript. One of us (K.W.) thanks Stanford University for its hospitality during his visit there. This work was supported by the U.S. National Science Foundation through NSF-ECS (Electronic Circuits and Systems) and NSF-DMR (Division of Materials Research).

[1]B. D. Josephson, Phys. Lett. **1**, 251 (1962).
[2]T. D. Clark, Phys. Lett. **27A**, 585 (1968).
[3]A. K. Jain, K. K. Likharev, J. E. Lukens, and J. E. Sauvageau, Phys. Rep. **109**, 310 (1984).
[4]D. R. Tilley, Phys. Lett. **33A**, 205 (1970).
[5]V. N. Belykh, N. F. Pederson, and O. H. Soerensen, Phys. Rev. B **16**, 4860 (1977).
[6]K. K. Likharev, *Dynamics of Josephson Junctions and Circuits* (Gordon and Breach, New York, 1986).
[7]T. Van Duzer and C. W. Turner, *Principles of Superconductive Devices and Circuits* (Elsevier, New York, 1981), p. 170.
[8]W. Magnus and S. Winkler, *Hill's Equation* (Dover, New York, 1979).
[9]N. N. Bogoliubov and I. A. Mitropolskii, *Asymptotic Methods in the Theory of Nonlinear Oscillations* (Hindustan, Delhi, 1961).
[10]G. S. Lee and S. E. Schwarz, J. Appl. Phys. **55**, 1035 (1984).
[11]J. Guckenheimer and P. Holmes, *Nonlinear Oscillations, Dynamical Systems, and Bifurcations of Vector Fields* (Springer-Verlag, New York, 1983).
[12]See for example, *Multiparameter Bifurcation Theory*, Contemporary Mathematics **56**, edited by M. Golubitsky and J. Guckenheimer (American Mathematical Society, Providence, 1986).
[13]P. Hadley and M. R. Beasley, Appl. Phys. Lett. **50**, 621 (1987).
[14]K. Wiesenfeld (unpublished).
[15]J. E. Sauvageau, A. K. Jain, and J. E. Lukens, Inter. J. Infrared Millimeter Waves **8**, 1281 (1987).
[16]R. L. Kautz, C. A. Hamilton, and F. L. Lloyd, IEEE Trans. **MAG-23**, 883 (1987).